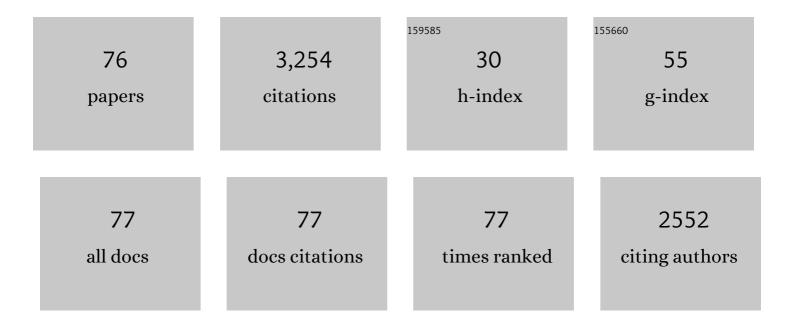
Thomas Wagner

List of Publications by Year in descending order

Source: https://exaly.com/author-pdf/4009967/publications.pdf Version: 2024-02-01



#	Article	IF	CITATIONS
1	GEM-SELEKTOR GEOCHEMICAL MODELING PACKAGE: TSolMod LIBRARY AND DATA INTERFACE FOR MULTICOMPONENT PHASE MODELS. Canadian Mineralogist, 2012, 50, 1173-1195.	1.0	375
2	An experimental study of the solubility and speciation of the Rare Earth Elements (III) in fluoride- and chloride-bearing aqueous solutions at temperatures up to 300°C. Geochimica Et Cosmochimica Acta, 2009, 73, 7087-7109.	3.9	311
3	GEM-Selektor geochemical modeling package: revised algorithm and GEMS3K numerical kernel for coupled simulation codes. Computational Geosciences, 2013, 17, 1.	2.4	148
4	A thermodynamic model for di-trioctahedral chlorite from experimental and natural data in the system MgO–FeO–Al2O3–SiO2–H2O: applications to P–T sections and geothermometry. Contribution To Mineralogy and Petrology, 2014, 167, 1.	n\$3.1	134
5	lron isotope fractionation during hydrothermal ore deposition and alteration. Geochimica Et Cosmochimica Acta, 2006, 70, 3011-3030.	3.9	125
6	MINERALS OF THE SYSTEM BI TE SE S RELATED TO THE TETRADYMITE ARCHETYPE: REVIEW OF CLASSIFICATION AND COMPOSITIONAL VARIATION. Canadian Mineralogist, 2007, 45, 665-708.	1.0	93
7	Negative Ce anomalies in Mn oxides: The role of Ce4+ mobility during water–mineral interaction. Geochimica Et Cosmochimica Acta, 2012, 86, 296-317.	3.9	84
8	Quantification of mixing processes in ore-forming hydrothermal systems by combination of stable isotope and fluid inclusion analyses. Geochimica Et Cosmochimica Acta, 2006, 70, 965-982.	3.9	81
9	Fluid mixing forms basement-hosted Pb-Zn deposits: Insight from metal and halogen geochemistry of individual fluid inclusions. Geology, 2013, 41, 679-682.	4.4	78
10	Fluid mixing from below in unconformity-related hydrothermal ore deposits. Geology, 2014, 42, 1035-1038.	4.4	78
11	Gold upgrading in metamorphosed massive sulfide ore deposits: Direct evidence from laser-ablation–inductively coupled plasma–mass spectrometry analysis of invisible gold. Geology, 2007, 35, 775.	4.4	75
12	Thermodynamic modeling of non-ideal mineral–fluid equilibria in the system Si–Al–Fe–Mg–Ca–Na–K–H–O–Cl at elevated temperatures and pressures: Implications for hydrothermal mass transfer in granitic rocks. Geochimica Et Cosmochimica Acta, 2008, 72, 526-553.	3.9	75
13	Contrasting paleofluid systems in the continental basement: a fluid inclusion and stable isotope study of hydrothermal vein mineralization, Schwarzwald district, Germany. Geofluids, 2007, 7, 123-147.	0.7	74
14	Stable Isotope Constraints on Ore Formation at the San Rafael Tin-Copper Deposit, Southeast Peru. Economic Geology, 2009, 104, 223-248.	3.8	62
15	Laser combustion analysis of î´34S of sulfosalt minerals. Geochimica Et Cosmochimica Acta, 2002, 66, 2855-2863.	3.9	58
16	An experimental study of the aqueous solubility and speciation of Y(III) fluoride at temperatures up to 250°C. Geochimica Et Cosmochimica Acta, 2013, 123, 403-415.	3.9	57
17	Unusual rare earth element fractionation in a tin-bearing magmatic-hydrothermal system. Geology, 2011, 39, 295-298.	4.4	56
18	Stable isotope (B, H, O) and mineral-chemistry constraints on the magmatic to hydrothermal evolution of the VarutrÃ s k rare-element pegmatite (Northern Sweden). Chemical Geology, 2016, 421, 1-16.	3.3	56

#	Article	IF	CITATIONS
19	Apatite as a tracer of the source, chemistry and evolution of ore-forming fluids: The case of the Olserum-Djupedal REE-phosphate mineralisation, SE Sweden. Geochimica Et Cosmochimica Acta, 2019, 255, 163-187.	3.9	53
20	MINERALOGY, MINERAL COMPOSITIONS AND FLUID EVOLUTION AT THE WENZEL HYDROTHERMAL DEPOSIT, SOUTHERN GERMANY: IMPLICATIONS FOR THE FORMATION OF KONGSBERG-TYPE SILVER DEPOSITS. Canadian Mineralogist, 2007, 45, 1147-1176.	1.0	52
21	Internally consistent thermodynamic data for aqueous species in the system Na–K–Al–Si–O–H–Cl. Geochimica Et Cosmochimica Acta, 2016, 187, 41-78.	3.9	47
22	Gold concentrations in metamorphic fluids: A LA-ICPMS study of fluid inclusions from the Alpine orogenic belt. Chemical Geology, 2014, 385, 70-83.	3.3	44
23	Pyrite metamorphism in the devonian hunsruck slate of Germany: Insights from laser microprobe sulfur isotope analysis and thermodynamic modeling. Numerische Mathematik, 2006, 306, 525-552.	1.4	43
24	Fluid–rock interaction in autoliths of agpaitic nepheline syenites in the IlÃmaussaq intrusion, South Greenlandâ~†. Lithos, 2006, 91, 331-351.	1.4	43
25	Mineralogy of complex Co-Ni-Bi vein mineralization, Bieber deposit, Spessart, Germany. Mineralogical Magazine, 2002, 66, 385-407.	1.4	42
26	Major and trace-element composition and pressure–temperature evolution of rock-buffered fluids in low-grade accretionary-wedge metasediments, Central Alps. Contributions To Mineralogy and Petrology, 2013, 165, 981-1008.	3.1	38
27	Source and origin of active and fossil thermal spring systems, northern Upper Rhine Graben, Germany. Applied Geochemistry, 2012, 27, 1153-1169.	3.0	35
28	Microanalysis of Fluid Inclusions in Crustal Hydrothermal Systems using Laser Ablation Methods. Elements, 2016, 12, 323-328.	0.5	35
29	Red bed and basement sourced fluids recorded in hydrothermal Mn–Fe–As veins, Sailauf (Germany): A LA-ICPMS fluid inclusion study. Chemical Geology, 2014, 363, 22-39.	3.3	32
30	Late-metamorphic veins record deep ingression of meteoric water: A LA-ICPMS fluid inclusion study from the fold-and-thrust belt of the Rhenish Massif, Germany. Chemical Geology, 2013, 351, 134-153.	3.3	31
31	Chemical evolution of metamorphic fluids in the Central Alps, Switzerland: insight from <scp>LA</scp> â€ <scp>ICPMS</scp> analysis of fluid inclusions. Geofluids, 2016, 16, 877-908.	0.7	31
32	Fluid evolution of the Neoarchean Pampalo orogenic gold deposit (E Finland): Constraints from LA-ICPMS fluid inclusion microanalysis. Chemical Geology, 2017, 450, 96-121.	3.3	31
33	Major and trace element geochemistry of tourmalines from Archean orogenic gold deposits: Proxies for the origin of gold mineralizing fluids?. Ore Geology Reviews, 2017, 91, 906-927.	2.7	31
34	An internally consistent thermodynamic dataset for aqueous species in the system Ca-Mg-Na-K-Al-Si-O-H-C-Cl to 800 °C and 5 kbar. Numerische Mathematik, 2017, 317, 755-806.	1.4	30
35	Laser microprobe sulphur isotope analysis of arsenopyrite: experimental calibration and application to the Boliden Au–Cu–As massive sulphide deposit. Ore Geology Reviews, 2004, 25, 311-325.	2.7	29
36	Formation of kyanite–quartz veins of the Alpe Sponda, Central Alps, Switzerland: implications for Al transport during regional metamorphism. Contributions To Mineralogy and Petrology, 2008, 156, 689-707.	3.1	28

THOMAS WAGNER

#	Article	IF	CITATIONS
37	The role of the Kupferschiefer in the formation of hydrothermal base metal mineralization in the Spessart ore district, Germany: insight from detailed sulfur isotope studies. Mineralium Deposita, 2010, 45, 217-239.	4.1	28
38	A magmatic source of hydrothermal sulfur for the Prominent Hill deposit and associated prospects in the Olympic iron oxide copper-gold (IOCG) province of South Australia. Ore Geology Reviews, 2017, 89, 1058-1090.	2.7	27
39	GEMSFITS: Code package for optimization of geochemical model parameters and inverse modeling. Applied Geochemistry, 2015, 55, 28-45.	3.0	26
40	EVOLUTION OF SULFIDE MINERALIZATION IN FERROCARBONATITE, SWARTBOOISDRIF, NORTHWESTERN NAMIBIA: CONSTRAINTS FROM MINERAL COMPOSITIONS AND SULFUR ISOTOPES. Canadian Mineralogist, 2006, 44, 877-894.	1.0	24
41	The Porphyry Cu-(Mo-Au) Deposit at Altar (Argentina): Tracing Gold Distribution by Vein Mapping and LA-ICP-MS Mineral Analysis. Economic Geology, 2014, 109, 1341-1358.	3.8	24
42	A new aqueous activity model for geothermal brines in the system Na-K-Ca-Mg-H-Cl-SO4-H2O from 25 to 300°C. Chemical Geology, 2014, 381, 78-93.	3.3	24
43	Barite-pyrite mineralization of the Wiesbaden thermal spring system, Germany: a 500-kyr record of geochemical evolution. Geofluids, 2005, 5, 124-139.	0.7	21
44	Fluid-rock interaction during formation of metamorphic quartz veins: A REE and stable isotope study from the Rhenish Massif, Germany. Numerische Mathematik, 2010, 310, 645-682.	1.4	21
45	Combined LA-ICP-MS microanalysis of iodine, bromine and chlorine in fluid inclusions. Journal of Analytical Atomic Spectrometry, 2018, 33, 768-783.	3.0	21
46	Hematite Breccia-Hosted Iron Oxide Copper-Gold Deposits Require Magmatic Fluid Components Exposed to Atmospheric Oxidation: Evidence from Prominent Hill, Gawler Craton, South Australia. Economic Geology, 2018, 113, 597-644.	3.8	21
47	Hydrogen isotope determination of fluid inclusion water from hydrothermal fluorite: Constraining the effect of the extraction technique. Chemical Geology, 2007, 244, 474-482.	3.3	20
48	Chemical evolution and origin of the LuumÃki gem beryl pegmatite: Constraints from mineral trace element chemistry and fractionation modeling. Lithos, 2017, 274-275, 147-168.	1.4	20
49	Metamorphic ore remobilization in the HÇefors district, Bergslagen, Sweden: constraints from mineralogical and small-scale sulphur isotope studies. Mineralium Deposita, 2005, 40, 100-114.	4.1	19
50	Magmatic-hydrothermal evolution of an unusual Mo-rich carbonatite: a case study using LA-ICP-MS fluid inclusion microanalysis and He–Ar isotopes from the Huangshui'an deposit, Qinling, China. Mineralium Deposita, 2021, 56, 1133-1150.	4.1	18
51	Lead isotope systematics of vein-type antimony mineralization, Rheinisches Schiefergebirge, Germany: a case history of complex reaction and remobilization processes. Mineralium Deposita, 2002, 37, 185-197.	4.1	16
52	Sulphur isotope geochemistry of black shale-hosted antimony mineralization, Arnsberg, northern Rhenish Massif, Germany: implications for late-stage fluid flow during the Variscan orogeny. Journal of the Geological Society, 2003, 160, 299-308.	2.1	14
53	Origin of the high-temperature Olserum-Djupedal REE-phosphate mineralisation, SE Sweden: A unique contact metamorphic-hydrothermal system. Ore Geology Reviews, 2018, 101, 740-764.	2.7	14
54	Stable isotope-based modeling of the origin and genesis of an unusual Au–Ag–Sn–W epithermal system at Cirotan, Indonesia. Chemical Geology, 2005, 219, 237-260.	3.3	13

THOMAS WAGNER

#	Article	IF	CITATIONS
55	Evolution of unconformity-related MnFeAs vein mineralization, Sailauf (Germany): Insight from major and trace elements in oxide and carbonate minerals. Ore Geology Reviews, 2013, 50, 28-51.	2.7	13
56	Volumetric Properties of Mixed Electrolyte Aqueous Solutions at Elevated Temperatures and Pressures. The Systems CaCl ₂ –NaCl–H ₂ O and MgCl ₂ –NaCl–H ₂ O to 523.15 K, 70 MPa, and lonic Strength from (0.1 to 18) mol·kg ^{–1} . Journal of Chemical & Engineering Data, 2014, 59, 2570-2588.	1.9	13
57	Magmatic-hydrothermal evolution of the Kymi topaz granite stock, SE Finland: Mineral chemistry evidence for episodic fluid exsolution. Lithos, 2017, 292-293, 401-423.	1.4	13
58	Fluid inclusion evidence for the magmatic-hydrothermal evolution of closely linked porphyry Au, porphyry Mo, and barren systems, East Qinling, China. Bulletin of the Geological Society of America, 2022, 134, 1529-1548.	3.3	13
59	Fluorite as indicator mineral in iron oxide-copper-gold systems: explaining the IOCG deposit diversity. Chemical Geology, 2020, 548, 119674.	3.3	12
60	Post-Variscan hydrothermal vein mineralization, Taunus, Rhenish Massif (Germany): Constraints from stable and radiogenic isotope data. Ore Geology Reviews, 2012, 48, 239-257.	2.7	11
61	Mineralogy, paragenesis, and mineral chemistry of REEs in the Olserum-Djupedal REE-phosphate mineralization, SE Sweden. American Mineralogist, 2018, 103, 125-142.	1.9	11
62	Textural evolution and trace element chemistry of hydrothermal calcites from Archean gold deposits in the Hattu schist belt, eastern Finland: Indicators of the ore-forming environment. Ore Geology Reviews, 2019, 112, 103006.	2.7	11
63	Sulphur isotope characteristics of recrystallisation, remobilisation and reaction processes: a case study from the Ramsbeck Pb-Zn deposit, Germany. Mineralium Deposita, 2001, 36, 670-679.	4.1	10
64	Fluid–rock interaction processes related to hydrothermal vein-type mineralization in the Siegerland district, Germany: implications from inorganic and organic alteration patterns. Applied Geochemistry, 2002, 17, 225-243.	3.0	9
65	Fluid–rock reactions in the 1.3ÂGa siderite carbonatite of the GrÃุnnedal–Ãka alkaline complex, Southwest Greenland. Contributions To Mineralogy and Petrology, 2018, 173, 1.	3.1	9
66	Mineral reactions in sulphide systems as indicators of evolving fluid geochemistry – a case study from the Apollo mine, Siegerland, FRG. Mineralogical Magazine, 1997, 61, 573-590.	1.4	8
67	Numerical Simulation of Reactive Fluid Flow on Unstructured Meshes. Transport in Porous Media, 2016, 112, 283-312.	2.6	8
68	Fluid Evolution of the Monte Mattoni Mafic Complex, Adamello Batholith, Northern Italy: Insights from Fluid Inclusion Analysis and Thermodynamic Modeling. Journal of Petrology, 2017, 58, 1645-1670.	2.8	8
69	The role of magmatic and hydrothermal processes in the formation of miarolitic gem beryl from the LuumĀki pegmatite, SE Finland. European Journal of Mineralogy, 2019, 31, 507-518.	1.3	7
70	Calcite trace element geochemistry of Au deposits in the Singu-Tabeikkyin Gold District, Myanmar: Implications for the sources of ore-forming fluids. Ore Geology Reviews, 2022, 145, 104892.	2.7	7
71	Mass transfer and fluid evolution in late-metamorphic veins, Rhenish Massif (Germany): insight from alteration geochemistry and fluid-mineral equilibria modeling. Mineralogy and Petrology, 2016, 110, 515-545.	1.1	6
72	From a F-rich granite to a NYF pegmatite: Magmatic-hydrothermal fluid evolution of the Kymi topaz granite stock, SE Finland. Lithos, 2020, 364-365, 105538.	1.4	6

#	Article	IF	CITATIONS
73	GEMSFIT: a generic fitting tool for geochemical activity models. Computational Geosciences, 2014, 18, 227-242.	2.4	5
74	Late-stage fluid exsolution and fluid phase separation processes in granitic pegmatites: Insights from fluid inclusion studies of the LuumA k i gem beryl pegmatite (SE Finland). Lithos, 2021, 380-381, 105852.	1.4	4
75	Telluride-bearing Au-Ag mineralization in the Singu-Tabeikkyin gold District, Mogok metamorphic Belt, Myanmar: New constraints on an intermediate-sulfidation epizonal orogenic ore system. Journal of Asian Earth Sciences, 2022, 227, 105120.	2.3	2
76	Halogen ratios in crustal fluids through time—Proxies for the emergence of aerobic life?. Geology, 0,	4.4	1